Am J Transl Res 2020;12(3):1070-1079
www.ajtr.org /ISSN:1943-8141/AJTR0102422

Original Article

Three-dimensional-printed titanium alloy porous scaffold combined with trans-cinnamaldehyde for repairing osteonecrosis of the femoral head in a dog model

Runzi Gao[1], Wenhui Ji[1], Tianwei Xia[1], Yanxing Fan[1], Wei Wei[1], Le Shi[1], Jinzhu Liu[1], Chao Zhang[1], Lezhen Xue[2], Jirong Shen[1]

[1]Affiliated Hospital of Nanjing University of Chinese Medicine, Nanjing 210029, Jiangsu, China; [2]Jiangsu Center for Safety Evaluation of Drugs, Nanjing 211816, Jiangsu, China

Received September 17, 2019; Accepted March 14, 2020; Epub March 15, 2020; Published March 30, 2020

Abstract: Osteonecrosis of the femoral head (ONFH) is a common disorder that may be idiopathic, caused by trauma, or associated with alcohol or glucocorticoid use. The goals of early treatment include delaying or avoiding hip replacement, but there are no effective treatments for early-stage disease. The aim of the present study was to evaluate the effects of treatment with 3D-printed porous titanium alloy scaffold combined with daily intraperitoneal trans-cinnamaldehyde (TCA) in a dog model of ONFH. Four weeks after creation of the ONFH model, MRI examination of the femoral head showed the characteristic "double line sign" of ONFH, verifying the validity of our model. After another 12 weeks, femoral head specimens were harvested and examined by gross inspection; micro-computed tomography; histologic staining (hematoxylin and eosin; Masson); immunohistochemical analysis and quantitative real-time polymerase chain reaction analysis. Gross inspection of the femoral head in untreated ONFH animals at 16 weeks after model creation showed pale, exfoliating articular cartilage and disordered trabecular bone. Treatment with 3D-printed titanium alloy porous scaffold combined with TCA ameliorated the pathologic ONFH changes and significantly reduced inmature bone tissue as well as imature collagen in the femoral head, as shown by Masson staining. This treatment also increased VEGF, BMP2, β-catenin, b-FGF, and RUNX2 expression and decreased PPARγ expression, compared with untreated ONFH. In conclusion, 3D-printed titanium alloy porous scaffold combined with TCA can effectively improve ONFH, which may be related to local repair. This provides the theoretical basis for a new treatment strategy for ONFH.

Keywords: Osteonecrosis of the femoral head, micro-CT, trans-cinnamaldehyde, 3D-printing titanium alloy porous scaffold

Introduction

Osteonecrosis of the femoral head (ONFH) is a relatively common disorder that most frequently occurs in men aged 30-50 years [1]. Approximately 20 million people worldwide and 8.12 million people in China have ONFH [2]. The duration of ONFH varies from a few months to several years and generally follows the pattern of "ischemia-necrosis-collapse", eventually leading to partial or complete loss of hip function [3]. The disability rate of ONFH is high, accounting for 5%-12% of all patients undergoing total hip arthroplasty [4]. There are several major risk factors for ONFH, including trauma, long-term or high-dose use of glucocorticoids, and long-term heavily intake of alcohol; in other instances, ONFH is idiopathic [5]. However, the exact etiology and pathogenesis of ONFH remain unclear.

The prevailing hypothesis of the pathogenesis of ONFH is a "multiple hit theory", which suggests that a pathogenic factor indirectly affects osteocytes by interfering with their blood supply, leading to cell damage and necrosis [6]. Before collapse of the femoral head, treatments focus on providing structural support for the head to promote bone regeneration, reduce pain, improve hip function, preserve the shape

of the femoral head, and delay hip replacement [7]. Core decompression is one treatment option for patients with early ONFH, but the effectiveness of this procedure alone is limited. Therefore, new strategies, such as vascular free iliac bone graft and platelet-rich plasma transplantation, have been used to complement core decompression [8]. However, these techniques may produce additional surgical trauma or require complex separation and purification procedures. Therefore, it is important to develop an implant for core decompression that has good mechanical properties and biocompatibility, is biologically active, and induces osteogenesis.

As the main component of the volatile oil of cinnamon, trans-cinnamaldehyde (TCA) exerts many pharmacological effects, including antiviral [9], anti-oxidation, anti-inflammatory [10], hypoglycemic, and anti-tumor activity [11]. Recent studies have shown that TCA can inhibit the formation of osteoclast-like cells [12]. Moreover, studies have demonstrated that TCA has dose-dependent effects on osteoblast proliferation and osteogenesis [13, 14]. TCA can also improve the microstructure of bone tissue and improve its biomechanical properties [15]. However, the effects of TCA on ONFH have rarely been reported, and its role and mechanism remain unclear.

In this study, we used 3-dimensional (3D) printing technology to prepare porous titanium alloy scaffolds with a stable mechanical structure, suitable pore size, high porosity, and an elastic modulus matching that of normal bone tissue. Systemic TCA was concurrently administered to promote osteogenesis, and a bioactive porous structure was constructed. Titanium alloy implants provide a new option for treating ONFH by promoting both mechanical and biological reconstruction.

Materials and methods

Reagents and materials

A customized 3D-printed titanium alloy porous scaffold (3DP-scaffold, P1253) was created using electron beam melting (EBM) 3D-printing technology, based on computed tomography and 3D model data. A porous titanium scaffold was designed. The 3D structure of the scaffold was designed using computer assisted design (CAD) software (Magics), and the data were stored in STL file format. The porous architecture was based on a dodecahedron unit cell with a pore size of approximately 600 μm, strut diameter of approximately 500 μm, and porosity of approximately 70%. This architecture was adopted because pore sizes in this range are beneficial for in-growth of bone and vessels. The implants were prototyped using the EBM Q10 system (Arcam AB, Sweden).

TCA (L1704064) was purchased from Aladdin Bio-Chem Technology (Shanghai, China). Immunohistochemistry analyses were performed using the following antibodies, which were obtained from Bioss Antibodies (Beijing, China): vascular endothelial growth factor (VEGF; bs-1665R), bone morphogenetic protein 2 (BMP2; bs-1012R), peroxisome proliferator-activated receptor γ (PPARγ; bs-0530R), β-catenin (bs-1165R), basic fibroblast growth factor (b-FGF; bs-2235R), and Runt-related transcription factor 2 (RUNX2; bs-1134R).

Grouping of experimental animals

Thirty male beagle dogs, weighing approximately 10 kg, were purchased from Nanjing Chaimen Biotechnology Co., Ltd. (Nanjing, China, SCXK (Su) 2016-0007). They were divided into five groups (n=6): control group, ONFH group, iliac bone graft (IBG) group, IBG+3DP-scaffold, and IBG+3DP-scaffold+TCA group.

Construction of the canine ONFH model

The animals were anesthetized and placed on the operating table with their limbs secured. After shaving the operating area to remove hair, we disinfected the area with iodophor, applied a surgical towel (with a central hole), and marked the position of the acetabulum and femoral shaft. The incision began at the lower edge of the acetabulum and was extended caudally to expose the greater trochanter of the femur. The knee joint was then flexed and the hip joint was opened to expose the femoral head. Liquid nitrogen (100 mL) was injected into the tunnel around the femoral head for 8 minutes using a liquid nitrogen freezing gun, after which the area was rewarmed by injection of physiological saline at 37°C three times. The muscles and overlying tissues were then sutured together and a skin dressing was applied.

Treatment of canine ONFH with 3DP-scaffold and TCA

After exposing the iliac crest, we used a rongeur to obtain iliac crest tissue; we then removed the cortical bone, leaving only the cancellous bone for use as a bone graft. The femoral head was exposed as described above, and subsequent treatment depended on the group: ONFH group, no additional treatment; IBG group, implantation with autologous cancellous bone; IBG+3DP-scaffold group, implantation with 3DP-scaffold and autologous cancellous bone; and IBG+3DP-scaffold+TCA group, implantation with autologous cancellous bone and 3DP-scaffold, as well as intraperitoneal injection of 30 mg/kg TCA daily. Dead bone was removed from the necrotic area before insertion of the 3DP-scaffold or autologous bone.

Micro-computed tomography analysis

All dogs were sacrificed 12 weeks after the operation. Their femoral head tissues were removed, fixed in 4% formalin for 48 hours at 4°C, and then inspected visually and imaged using the micro-CT system (energy 70 kVp, threshold 220, current 114 μA, integration time 300 ms, Skyscan 1173; Skyscan, Kontich, Belgium). Bone regeneration and volume of new bone in the specimens were calculated using the system's software.

Histologic evaluation of canine femoral head specimens

The femoral head tissues were fixed in 4% paraformaldehyde, decalcified, embedded in paraffin, cut into 5-μm sections, and then stained with hematoxylin and eosin (H&E) and Masson stain. An optical microscope (Olympus, Japan) was used to observe histopathologic changes.

Immunohistochemistry

Immunohistochemical staining was used to detect expression of VEGF, BMP2, PPARγ, β-catenin, b-FGF, and RUNX2 in the femoral head tissues. Briefly, paraffin sections were deparaffinized, rehydrated, and then incubated in 3% hydrogen peroxide. The samples were incubated with the corresponding primary antibody at 4°C overnight after being blocked with 3% bovine serum albumin. They were subsequently incubated with secondary and tertiary antibodies for 20 minutes at 37°C. The samples were then stained with 3,3'-diaminobenzidine and restained with hematoxylin. After dehydration and drying, the sections were observed under a light microscope (200×) (Nikon, Tokyo, Japan) and analyzed with Image J software (National Institutes of Health, Bethesda, MD, USA).

Quantitative real-time polymerase chain reaction (qPCR)

Total RNA was extracted from femoral head tissues and reversed based on the protocol. qPCR was carried out according to the manufacturer's instructions. All data were quantified using the threshold cycle normalized to GAPDH. The primers used in the study were listed: RUNX2 forward: 5'-ATGAGAGTAGGTGTCCCGCC-3'; reverse: 5'-GGAGTGAATGGACGGGGATG-3; VEGF forward: 5'-GGCCTTTGGCCAAGTGATTG-3'; reverse: 5'-CGGTGTTCACTGTGTGTTGC-3'; BMP2 forward: 5'-CGGGGTACCACGCCTTTTAT-3'; reverse: 5'-CCACAACCCTCCACAACCAT-3'; β-catenin forward: 5'-AATCCTGTGTGGGGAATGGC-3'; reverse: 5'-GATGGTTCAGCCAAACGCTG-3'; PPARγ forward: 5'-CCTCTTCCATGCTGTTATGGGT-3'; reverse: 5'-GCAAGGCACTTCTGAAACCG-3'; GAPDH forward: 5'-CCCACTCTTCCACCTTCGAC-3'; reverse: 5'-GGTGGTCCAGGAGGCTCTTA-3'.

Statistical analysis

All data are expressed as mean ± standard deviation. Significant differences between groups were determined using unpaired Student's t-test, post-hoc Tukey's honestly significant difference test, and analysis of variance (ANOVA) (SPSS 22.0 software, Chicago, IL, USA). $P < 0.05$ was considered statistically significant.

Results

Verification of ONFH model by magnetic resonance imaging

All dogs underwent hip magnetic resonance imaging (MRI) to assess the validity of our model. Low signal intensity in T1-weighted images of the head or head-neck junction area and high signal intensity in T2-weighted images and fat-suppressed images were used as criteria to diagnose ONFH. T2-weighted images of

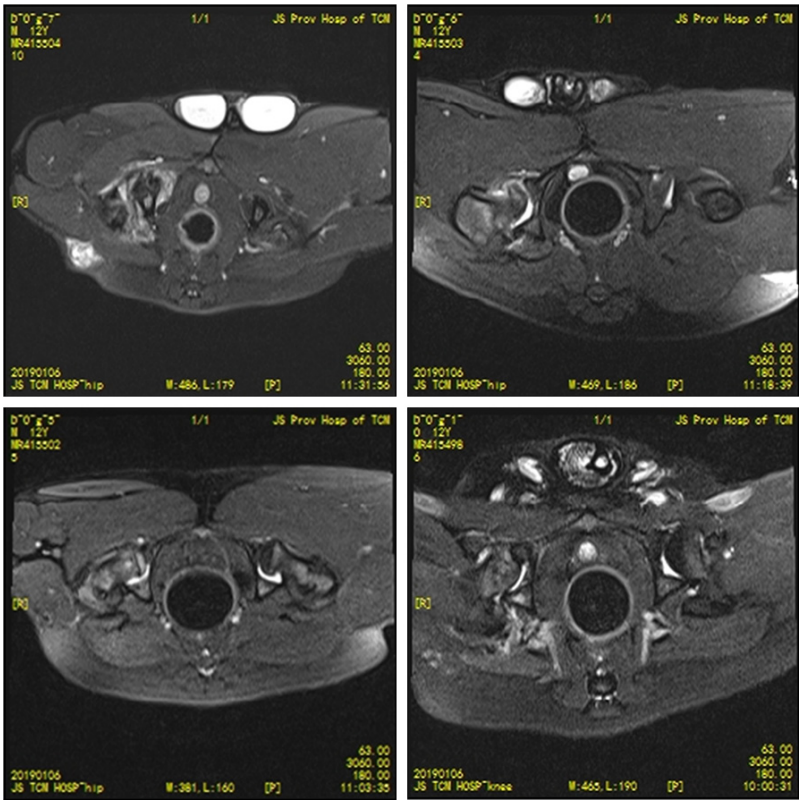

Figure 1. Magnetic resonance imaging of the hip joint in a dog model of osteonecrosis of the femoral head.

the femoral head showed an uneven high-intensity signal with the characteristic "double line sign" of ONFH, verifying successful establishment of an ONFH model (**Figure 1**).

Gross inspection

At 12 weeks after surgery, the femoral heads in the control group were round, with no evidence of collapse or fragmentation. The articular cartilage was smooth and of normal color. At the same time, the femoral heads in the ONFH group were irregular in shape and showed evidence of collapse. The articular cartilage was rough and pale (**Figure 2**).

Micro-computed tomography analysis

As shown in **Figure 3**, postoperative femoral head repair was most apparent in the IBG+3DP-scaffold+TCA group. In this group, the shape of the femoral head was round. In the IBG+3DP-scaffold group, the femoral head exhibited moderate repair, although it was slightly collapsed. In the IBG group, the results were poor: bone resorption, bone destruction, and trabecular bone fractures were observed, and there was prominent collapse of the femoral head. The ONFH group had severe bone resorption and destruction, with no apparent bone repair. These animals exhibited bone trabecular fractures, as well as severely deformed and collapsed femoral heads. Thus, all active treatment groups exhibited improved necrosis of the femoral head, with improvement being most obvious in the IBG+3DP-scaffold+TCA.

H&E staining

In the control group, the articular surface of the femoral head was smooth, and the structure and morphology were normal; the chondrocytes were arranged in an organized fashion (**Figure 4**). Trabecular bone in the femoral head was clear and complete, with a regular arrangement. There was no fat cell hyperplasia or hypertrophy, and there was a normal quantity of hematopoietic cells in the medullary cavity. In the ONFH group, bone destruction in the subchondral necrotic area was severe, and discontinuous bone fragments were observed. Trabecular bone was sparse, narrowed, and fractured. The number of bone cells in necrotic trabeculae was significantly reduced, and the number of empty bone lacuna was significantly increased. These H&E findings of necrosis in the femoral head were reduced in the active treatment groups, with the improvement being most obvious in the IBG+3DP-scaffold+TCA group.

Masson staining

In the control group, green and blue staining representing inmature bone tissue and collagen were rare; Masson staining was primarily red. Compared with the control group, the ONFH group showed a large quantity of blue-stained collagen in the trabecular bone and at the edges, and the inmature collagen area was

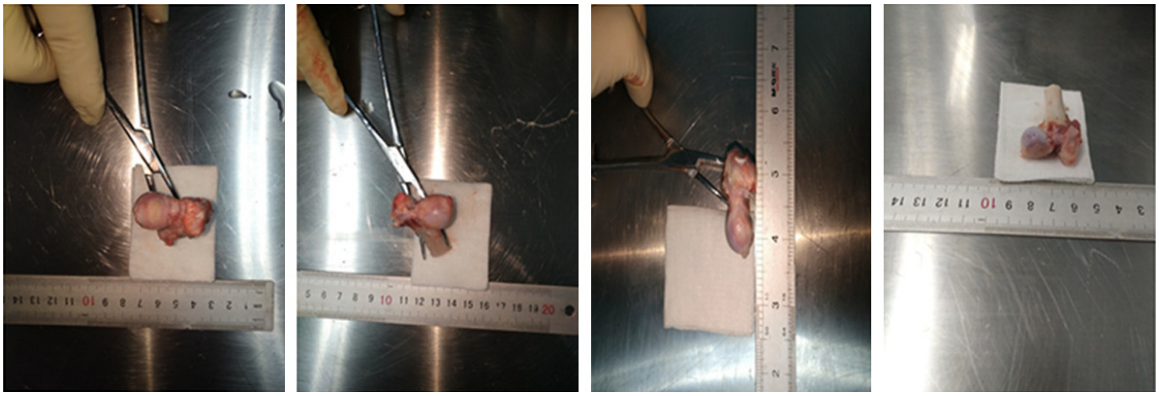

Figure 2. Gross inspection of the femoral head in a dog model of osteonecrosis of the femoral head. Disorders of femoral head subchondral bone trabeculae, uneven density, pale color, hardened bone formation.

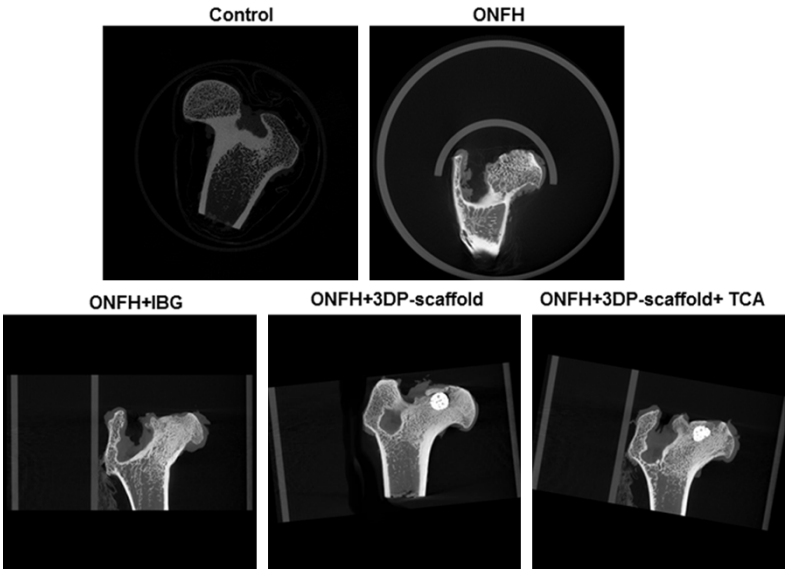

Figure 3. Effects of the 3DP-scaffold combined with TCA on micro-computed tomography results of the femoral head of dogs with osteonecrosis of the femoral head. The femoral heads were removed from the dogs at the end of experiment. 3DP-scaffold, 3-dimensional-printed scaffold; IBG, iliac bone graft; ONFH, osteonecrosis of the femoral head; TCA, trans-cinnamaldehyde.

significantly increased. Compared with the ONFH group, the active treatment groups exhibited significantly reduced area of inmature bone tissue (green and blue staining) and the tissue was mostly stained red (**Figure 5**). The area of blue-stained collagen was significantly decreased in the active treatment groups, especially in the IBG+3DP-scaffold+TCA group.

Immunohistochemistry

To investigate the mechanism of ONFH, we performed immunohistochemistry experiments to examine the expression of VEGF, BMP2, PPARγ, β-catenin, b-FGF, and RUNX2 in femoral head tissues. Compared with the control group, the ONFH group exhibited significantly decreased VEGF, BMP2, β-catenin, b-FGF, RUNX2 expression and significantly increased PPARγ expression (**Figures 6** and **7**). In the active treatment groups, expression of VEGF, BMP2, PPARγ, β-catenin, b-FGF, RUNX2 increased and expression of PPARγ decreased, compared with the ONFH group, with improvements being most pronounced in the IBG+3DP-scaffold+TCA group.

qPCR analysis

The mRNA expression of, β-catenin, PPARγ, RUNX2, VEGF, and BMP2 was consistent with the results of immunohistochemistry. The ONFH group significantly decreased the mRNA expression of β-catenin, RUNX2, VEGF, BMP2 and significantly increased PPARγ mRNA expression (**Figure 8**). In the active treatment groups, mRNA expression of β-catenin, RUNX2, VEGF, BMP2 increased and mRNA expression of PPARγ decreased, compared with the ONFH group, with improvements being most pronounced in the IBG+3DP-scaffold+TCA group.

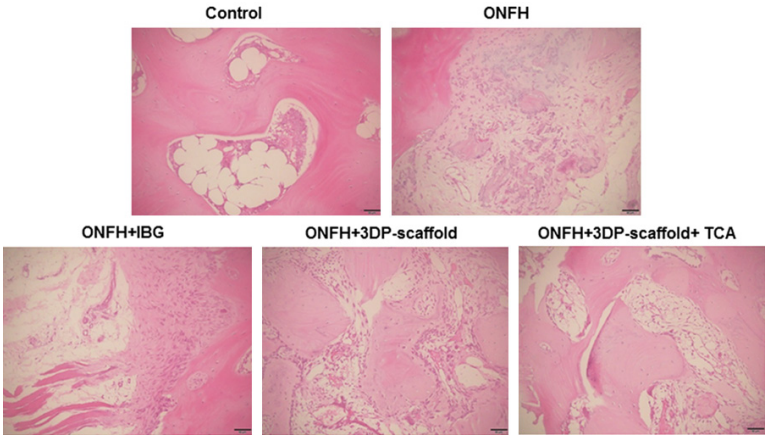

Figure 4. Effects of the 3DP-scaffold combined with TCA on histopathologic changes in the femoral head of dogs with osteonecrosis of the femoral head. The femoral heads were removed at the end of the experiment. 3DP-scaffold, 3-dimensional-printed scaffold; IBG, iliac bone graft; ONFH, osteonecrosis of the femoral head; TCA, trans-cinnamaldehyde.

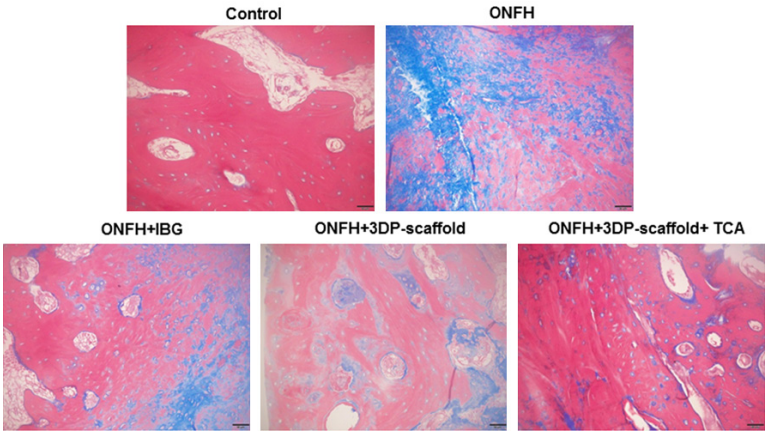

Figure 5. Effects of the 3DP-scaffold combined with TCA on Masson staining of the femoral head in dogs with osteonecrosis of the femoral head. The femoral heads were removed from the dogs for this analysis at the end of the experiment. 3DP-scaffold, 3-dimensional-printed scaffold; IBG, iliac bone graft; ONFH, osteonecrosis of the femoral head; TCA, trans-cinnamaldehyde.

Discussion

Titanium and its alloys have good mechanical load-bearing properties and biocompatibility and are one of the most widely used materials in clinical medicine [16]. At present, medical titanium metal prepared by conventional methods has poor biological activity, and its ability to guide bone tissue growth is unsatisfactory [17]. In addition, the traditional Ti-6Al-4V alloy has an elastic modulus of approximately 110 GPa, whereas the human body has an elastic modulus of approximately 20 GPa [18]. This difference in mechanical properties causes a stress shielding effect, which affects initial healing of the implant and long-term stability. To circumvent this problem, the alloy composition can be optimized: for example, the elastic modulus of the Ti-XNb alloy is as low as approximately 300 Pa [19]. It is also possible to construct a porous structure, thereby reducing the overall elastic modulus of the material. With the rapid development of 3D-printing technology, CAD can accurately control the structure and performance parameters of the supporting implant, such as its porosity, hole connectivity, aperture size, profile, and mechanical properties [20]. Porous titanium scaffolds can reach 80%-90% porosity, which not only reduces the elastic modulus of the alloy but also provides a good microenvironment for bone tissue regeneration and promotes the growth of bone tissue into the material [21, 22]. In this study, H&E and Masson staining, as well as micro-CT imaging, confirmed the effectiveness of the 3DP-scaffold for improving the pathologic changes associated with ONFH.

The main active ingredient of cinnamon is the volatile oil TCA. The results of a number of studies suggest that TCA is a potentially useful treatment strategy for ONFH. TCA may improve ONFH through several mechanisms: inhibition of the proliferation of fibroblasts, osteoclasts, and bone marrow mesenchymal stem cells; promotion of osteoblast proliferation; and enhancement of bone remodeling [23-25]. Abnormal proliferation of fibroblasts can promote degradation of the extracellular matrix and damage chondrocytes. Shi *et al.* found that high concentrations of TCA significantly inhibited the growth of fibroblasts in patients with osteoarthritis. Low con-

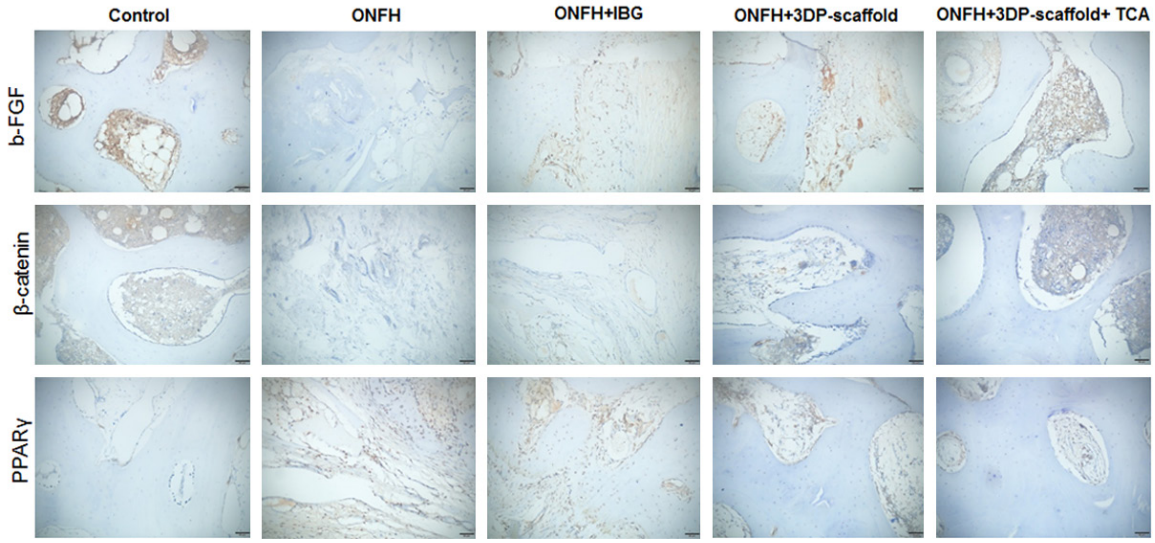

Figure 6. Immunohistochemistry results showing the effects of the 3DP-scaffold combined with TCA on the expression of b-FGF, β-catenin, and PPARγ in dogs with osteonecrosis of the femoral head. The femoral heads were removed from the dogs at the end of the experiment. 3DP-scaffold, 3-dimensional-printed scaffold; IBG, iliac bone graft; ONFH, osteonecrosis of the femoral head; TCA, trans-cinnamaldehyde.

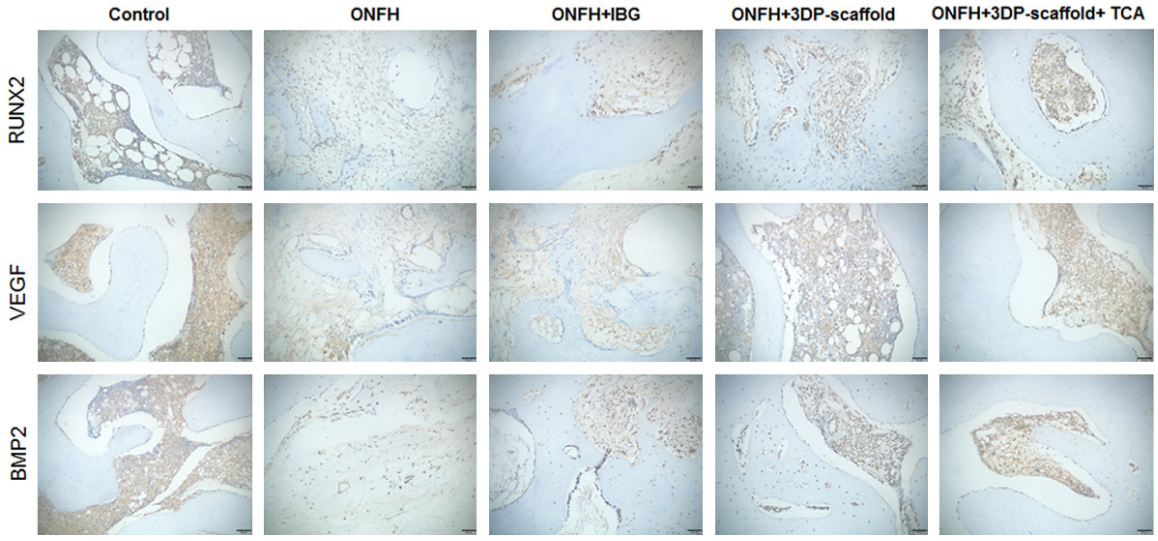

Figure 7. Immunohistochemistry results showing the effects of the 3DP-scaffold combined with TCA on the expression of RUNX2, VEGF, and BMP2 in dogs with osteonecrosis of the femoral head. The femoral heads were removed from the dogs at the end of the experiment. 3DP-scaffold, 3-dimensional-printed scaffold; IBG, iliac bone graft; ONFH, osteonecrosis of the femoral head; TCA, trans-cinnamaldehyde.

centrations of TCA can significantly increase osteoblast alkaline phosphatase activity, upregulate BMP-2 mRNA expression, and promote proliferation and differentiation of osteoblasts, thereby enhancing osteogenesis [26]. In the current study, combining TCA with the 3DP-scaffold and autologous bone produced the best therapeutic effects.

Osteonecrosis of the femoral head involves interruption of, or damage to, the blood supply to the femoral head, causing cell death and subsequent repair of bone cells and bone marrow cell components. This, in turn, leads to structural changes in the femoral head, collapse of this head, and joint dysfunction [27]. There are many causes of this common and dif-

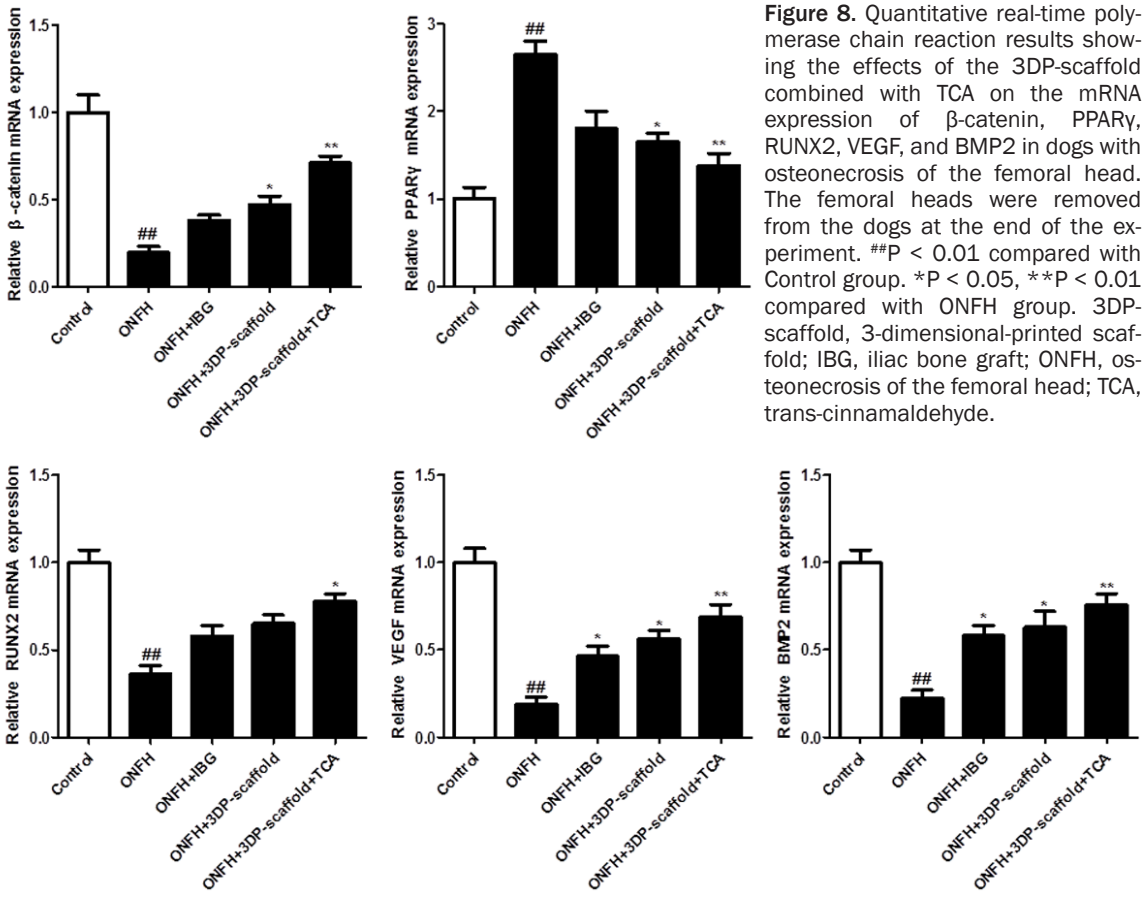

Figure 8. Quantitative real-time polymerase chain reaction results showing the effects of the 3DP-scaffold combined with TCA on the mRNA expression of β-catenin, PPARγ, RUNX2, VEGF, and BMP2 in dogs with osteonecrosis of the femoral head. The femoral heads were removed from the dogs at the end of the experiment. ##P < 0.01 compared with Control group. *P < 0.05, **P < 0.01 compared with ONFH group. 3DP-scaffold, 3-dimensional-printed scaffold; IBG, iliac bone graft; ONFH, osteonecrosis of the femoral head; TCA, trans-cinnamaldehyde.

ficult to treat disorder, and femoral neck fractures are more common when ONFH is caused by trauma, especially when the blood supply is damaged. However, the specific pathogenetic and molecular regulation mechanisms have not yet been clarified. At the molecular level, most recent research has focused on the regulation of transcription factors. In the present study, we used immunohistochemical analysis to examine the expression of VEGF, BMP2, PPARγ, β-catenin, b-FGF, and RUNX2 in ONFH. In the ONFH group, expression of VEGF, BMP2, β-catenin, b-FGF, and RUNX2 was greatly reduced, while PPARγ expression was significantly increased, when compared to control animals. These gene expression changes were reversed in the treatment groups.

Based on the above results, we conclude that the 3DP-scaffold implant combined with TCA can promote proliferation and differentiation of osteoblasts and inhibit proliferation of osteoclasts while providing structural support in an ONFH dog model. By upregulating VEGF to promote neovascularization, this treatment can be used as an innovative strategy for repairing bone defects associated with ONFH.

Disclosure of conflict of interest

None.

Address correspondence to: Jirong Shen, Affiliated Hospital of Nanjing University of Chinese Medicine, Nanjing 210029, Jiangsu, China. E-mail: joint66118@sina.com; Lezhen Xue, Jiangsu Center for Safety Evaluation of Drugs, Nanjing 211816, Jiangsu, China. E-mail: 1525794594@qq.com

References

[1] Kabata T, Maeda T, Tanaka K, Yoshida H, Kajino Y, Horii T, Yagishita S and Tsuchiya H. Hemi-resurfacing versus total resurfacing for osteonecrosis of the femoral head. J Orthop Surg 2011; 19: 177-180.

[2] Microsurgery Department of the Orthopedics Branch of the Chinese Medical Doctor Association; Group from the Osteonecrosis and Bone Defect Branch of the Chinese Association of Reparative and Reconstructive

Surgery; Microsurgery and Reconstructive Surgery Group of the Orthopedics Branch of the Chinese Medical Association. Chinese guideline for the diagnosis and treatment of osteonecrosis of the femoral head in adults. Orthop Surg 2017; 9: 3-12.

[3] Kaushik AP, Das A and Cui Q. Osteonecrosis of the femoral head: an update in year 2012. World J Orthop 2012; 3: 49-57.

[4] Mouzas OD, Zibis AH, Bonotis KS, Katsimagklis CD, Hadjigeorgiou GM, Papaliaga MN, Dimitroulias AP and Malizos KN. Psychological distress, personality traits and functional disability in patients with osteonecrosis of the femoral head. J Clin Med Res 2014; 6: 336.

[5] Fukushima W, Yamamoto T, Takahashi S, Sakaguchi M, Kubo T, Iwamoto Y and Hirota Y; Idiopathic ONFH Multicenter Case-Control Study. The effect of alcohol intake and the use of oral corticosteroids on the risk of idiopathic osteonecrosis of the femoral head: a case-control study in Japan. Bone Joint J 2013; 95-B: 320-325.

[6] Maniwa S, Nishikori T, Furukawa S, Kajitani K, Iwata A, Nishikawa U and Ochi M. Evaluation of core decompression for early osteonecrosis of the femoral head. Arch Orthop Trauma Surg 2000; 120: 241-4.

[7] Seyler TM. New treatment approaches for osteonecrosis of the femoral head: an overview. Instr Course Lect 2007; 56: 197-212.

[8] Cao H, Guan H, Lai Y, Ling Q and Wang X. Review of various treatment options and potential therapies for osteonecrosis of the femoral head. J Orthop Transl 2016; 4: 57-70.

[9] Hayashi K, Imanishi N, Kashiwayama Y, Kawano A, Terasawa K, Shimada Y and Ochiai H. Inhibitory effect of cinnamaldehyde, derived from cinnamomi cortex, on the growth of influenza A/PR/8 virus in vitro and in vivo. Antiviral Res 2007; 74: 1-8.

[10] Kim ME, Na JY and Lee JS. Anti-inflammatory effects of trans-cinnamaldehyde on lipopolysaccharide-stimulated macrophage activation via MAPKs pathway regulation. Immunopharmacol Immunotoxicol 2018; 40: 219-224.

[11] Zhang LQ, Zhang ZG, Fu Y, Xu Y. [Research progress of trans-cinnamaldehyde pharmacological effects]. Zhongguo Zhong Yao Za Zhi 2015; 40: 4568-72.

[12] Tsuji-Naito K. Aldehydic components of cinnamon bark extract suppresses RANKL-induced osteoclastogenesis through NFATc1 downregulation. Bioorg Med Chem 2008; 16: 9176-9183.

[13] Weng SJ, Yan DY, Tang JH, Shen ZJ, Wu ZY, Xie ZJ, Yang JY, Bai BL, Chen L, Boodhun V, Yang L, Da Eric Dong X and Yang L. Combined treatment with Cinnamaldehyde and beta-TCP had an additive effect on bone formation and angiogenesis in critical size calvarial defect in ovariectomized rats. Biomed Pharmacother 2019; 109: 573-581.

[14] Xu P and Chen CJ. [The effect of shifting of estrogen level on the expression of estrogen receptor and morphology of condyle in rat]. Shanghai Kou Qiang Yi Xue 2016; 25: 266-270.

[15] Dewi AH, Ana ID and Jansen J. Preparation of a calcium carbonate-based bone substitute with cinnamaldehyde crosslinking agent with potential anti-inflammatory properties. J Biomed Mater Res A 2017; 105: 1055-1062.

[16] Zhuang Y, Shang XW, Zhang H, Liu M and Xu SE; Orthopedics DO. Implant fixation with titanium alloy repairs spinal tuberculosis: its biocompatibility and mechanical properties. Chinese Journal of Tissue Engineering Research 2016.

[17] Terabe K, Kato K, Miyazaki H, Yamaguchi S, Imai A and Iguchi Y. Microstructure and crystallization behaviour of TiO 2 precursor prepared by the sol-gel method using metal alkoxide. Journal of Materials Science 1994; 29: 1617-1622.

[18] Olsen RH and Moreen HA. Calculation of the elastic anisotropy of Ti:6Al-4V alloy sheet from pole figure data. Metallurgical Transactions 1973; 4: 701-705.

[19] Kim WY, Kim HS and Yeo ID. Low elastic modulus β Ti-Nb-Si alloys for biomedical applications. Materials Science Forum 2006; 510-511: 858-861.

[20] Farzadi A, Waran V, Solati-Hashjin M, Rahman ZAA, Asadi M and Osman NAA. Effect of layer printing delay on mechanical properties and dimensional accuracy of 3D printed porous prototypes in bone tissue engineering. Ceramics International 2015; 41: 8320-8330.

[21] Torressanchez C, Fra AM, Norrito M, Yendall K, Liu Y and Conway PP. The effect of pore size and porosity on mechanical properties and biological response of porous titanium scaffolds. Mater Sci Eng C Mater Biol Appl 2017; 77: 219-228.

[22] El-Hajje A, Kolos EC, Wang JK, Maleksaeedi S, He Z, Wiria FE, Choong C and Ruys AJ. Physical and mechanical characterisation of 3D-printed porous titanium for biomedical applications. J Mater Sci Mater Med 2014; 25: 2471-2480.

[23] Wu Z, Yan D, Xie Z, Weng S, Zhou Q, Li H, Bai B, Boodhun V, Shen Z, Tang J and Yang L. Combined treatment with cinnamaldehyde and PTH enhances the therapeutic effect on glucocorticoid-induced osteoporosis through inhibiting osteoclastogenesis and promoting osteoblastogenesis. Biochem Biophys Res Commun 2018; 505: 945-950.

[24] Mateen S, Rehman MT, Shahzad S, Naeem SS, Faizy AF, Khan AQ, Khan MS, Husain FM and Moin S. Anti-oxidant and anti-inflammatory effects of cinnamaldehyde and eugenol on mononuclear cells of rheumatoid arthritis patients. Eur J Pharmacol 2019; 852: 14-24.

[25] Xia T, Gao R, Zhou G, Liu J, Li J and Shen J. Trans-cinnamaldehyde inhibits IL-1beta-stimulated inflammation in chondrocytes by suppressing NF-kappaB and p38-JNK pathways and exerts chondrocyte protective effects in a rat model of osteoarthritis. Biomed Res Int. 2019; 2019: 4039472.

[26] Shi X, Wu J, Wang Q, Zhao J, Yang L and Zhang D. Effects of cinnamaldehyde on proliferation of synovial fibroblasts in human knee osteoarthritis. Chinese Journal of Traditional Medical Traumatology & Orthopedics 2014; 1-3.

[27] Bachiller FG, Caballer AP and Portal LF. Avascular necrosis of the femoral head after femoral neck fracture. Clin Orthop Relat Res 2002; 87-109.